PAPER

New cationic coinage metal complexes featuring silyl group functionalized phosphine: syntheses, structures and catalytic studies in alkyne–azide cycloaddition reactions†

Amiya Kumar Sahoo,[a] Ashish Kumar Sahoo,[a] Bhagyashree Das,[a] Subhra Jyoti Panda,[b] Chandra Shekhar Purohit [ID][b] and Adinarayana Doddi [ID] *[a]

A series of coinage metal complexes bearing rarely explored *ortho*-silylated phosphine is reported. The treatment of diphenyl(2-(trimethylsilyl)phenyl)phosphine (**1**) with CuCl and $[Cu(CH_3CN)_4]BF_4$ furnished the corresponding neutral $[(\mathbf{1})CuCl]_2$ (**2**) and mono-cationic $[(\mathbf{1})_2Cu(CH_3CN)]BF_4$ (**3**) complexes, respectively. The reactions of **1** with AgX (X = BF_4^-, NO_3^-) in 2 : 1 ratio furnished the corresponding mono cationic dicoordinate silver(I) complexes of the type $[(\mathbf{1})_2Ag]X$ (X = BF_4^- (**4a**), NO_3^- (**4b**)). The *ortho*-silylated phosphine ligand (**1**) was conveniently converted into the corresponding sulfide (**5a**) and selenide (**5b**) species, and their reactions with $[Cu(CH_3CN)_4]BF_4$ yielded mono-cationic, homoleptic tris(silylphosphinochalcogenide)copper(I) complexes of the type $[(\mathbf{5a/5b})_3Cu]BF_4$ (**6a/6b**). The molecular structures of **2–4** and **6** were established by single-crystal X-ray diffraction analysis. The copper complexes **2**, **3**, and **6a** were employed as catalysts in azide–alkyne cycloaddition reactions. Among these complexes, **3** was extensively used in the preparation of various mono- and bis-triazoles consisting of tolyl, benzyl, carbazolyl, and propargylic ether groups. Three sets of substituted triazole derivatives were achieved under mild conditions by employing copper(I) catalytic systems. The mechanistic studies indicated the formation of a heteroleptic copper(I) triazolide intermediate which was detected by high-resolution mass spectral analysis.

Introduction

Over the last two decades, the organometallic chemistry community has witnessed tremendous developments in the design and isolation of stereoelectronically tuneable ligands featuring various phosphine groups and their applications in the stabilization and isolation of novel metal complexes.[1] It is noteworthy that phosphine ligands functionalized with Lewis acidic moieties such as the group 13 and 14 elements in their +3 and +4 oxidation states, respectively, have been widely explored in coordination and organometallic chemistry as *ambiphilic ligands* (Chart 1).[2,3] This type of ligand stabilizes

metal centers in an intramolecular fashion in two different bonding modes, namely by donor atoms from the Lewis basic center and a simultaneous back donation from the metal atoms to the Lewis acidic centers of the ligand. Therefore, such a class of ligand systems has been found to serve as

[a]Department of Chemical Sciences; Indian Institute of Science Education and Research Berhampur; Transit Campus, Industrial Training Institute (ITI); Engineering School Road, Ganjam, Odisha, 760010, India. E-mail: adoddi@iiserbpr.ac.in

[b]School of Chemical Sciences, National Institute of Science Education and Research (NISER), Bhubaneswar, 752050, India
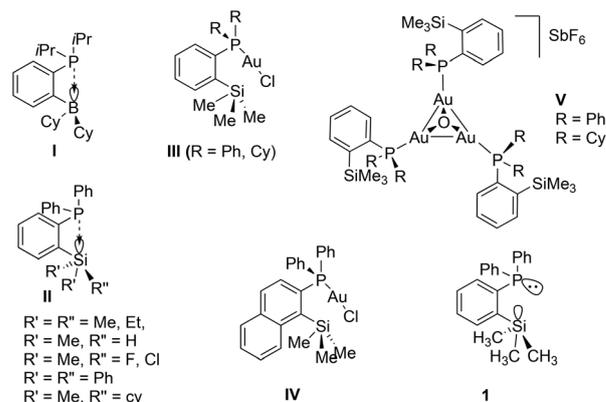
Chart 1 Examples of *ortho*-position substituted electronically modified phosphorus(III) compounds and their gold complexes (R = alkyl or aryl group).

effective ligands in electronic and steric tuning around the metal centres of interest to achieve specific properties such as inducing more electrophilic nature in well-defined and soluble transition metal catalysts in homogeneous catalytic pathways.[3,4] In this context, the notable examples of such type of reactive species can be considered from the pioneering reports by the group of Bourissou and co-workers.[5]

As shown in Chart 1, group 13 and 14 element substituted phosphines of types **I** and **II** were isolated and used in both main group and transition metal chemistry. Among these two classes of phosphines, type **I** was introduced recently;[6–8] however, species of type **II** (R = Me, Cl, H) were isolated several years ago.[9–11] Type **II** phosphines consisting of *ortho*-silylated groups and their transition metal complexes have been shown to exhibit enhanced solubility in various non-polar solvents which is in contrast to many typical aryl phosphine ligands.[4,12–14] Additionally, the type **II** species have also been employed as mono-dentate ligands in coinage metal chemistry,[15] for instance gold(I) chloride complexes of type **III** [(**II**[R]) AuCl] (R = Ph, Cy) and **IV** have been isolated.[15] Furthermore, the corresponding cationic complexes featuring trimetallic gold complexes of the type [{(**II**[R])Au}₃O]SbF₆ (**V**, R = Ph, Cy) have been isolated and structurally characterized. In a similar fashion, Shi and co-workers demonstrated the isolation of gold (I) chloride complexes of type **III**.[11]

In view of the general interest, various phosphines functionalized with group 13[6,7,16] and 14 element-containing groups (as Lewis acidic moieties) as monodentate ligands[17] have not been studied extensively in transition metal organometallic chemistry and homogeneous catalysis as in the case of their pincer counterparts (PSiP).[2,3,18] Their transition metal chemistry is still in its infancy. These systems can be considered as more electron rich species; in addition, they can provide high solubility to their metal complexes compared to classical triphenylphosphines. In this contribution, we wish to report the synthesis and structural characterization of a series of coinage metal(I) complexes (Cu and Ag) bearing monodentate phosphine (**1**) and copper complexes of sulfides and selenides of **1**. In addition, one of the bis(phosphine)copper(I) complexes was introduced as a catalyst in the synthesis of various substituted simple to complex triazole derivatives in good to high yields.

Results and discussion

The *ortho*-silylated phosphine **1** was prepared as a colourless oily substance by a slightly modified synthetic procedure.[10] As shown in Scheme 1, the *in situ* generated lithium salt was treated with trimethylchlorosilane at 0 °C, and the crude product was purified by silica gel column chromatography. The spectroscopic (¹H, ¹³C, and ³¹P NMR) and CHNS data were similar to the reported data.[10]

Single crystals suitable for X-ray diffraction analysis were grown by slow evaporation of *n*-hexane solution at RT. The molecular structure is similar to those that have been established for similar phosphine ligands (Fig. 1). For instance, the
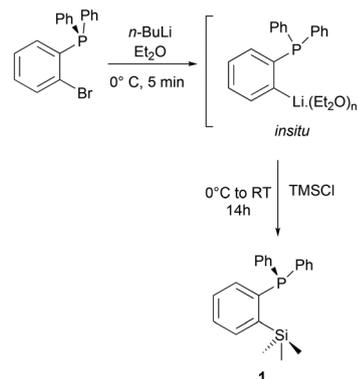
Scheme 1 Preparation of compound **1** from bromophenyldiphenylphosphine.
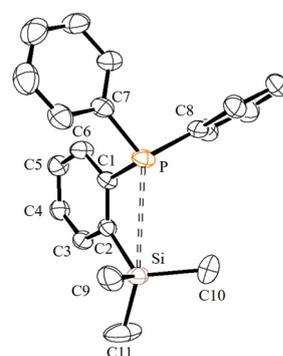
Fig. 1 ORETP view of one of the two molecules of **1** in the crystal lattice showing 30% ellipsoid probability. Hydrogen atoms are omitted for clarity. Important bond lengths [Å] and angles [°]: P–C1 1.846(2), P⋯Si 3.381, C1–C2 1.411(3), C2–Si 1.894(2), C7–P–C8 102.57(11), and C9–Si–C10 110.65(16).

average P⋯Si separation in **1** is about 3.39 Å which is in the range observed for the reported P⋯Si separation (3.31 Å) in *ortho*-diisopropyl chlorosilyl-functionalized triarylphosphane.[9]

Preparation and characterization of copper(I) and silver(I) cationic and neutral complexes bearing 1

The reactivity of *ortho*-silylated phosphine **1** was studied towards various copper and silver metal precursors (Scheme 2). The treatment of **1** with copper(I) chloride in THF at 60 °C afforded the neutral complex [(**1**)₂CuCl]₂ (**2**) as a pale-yellow solid in 87% yield, whereas the phosphine and cationic copper sources [Cu(CH₃CN)₄]BF₄ or AgX (X = BF₄⁻, or NO₃⁻) in a 2:1 ratio in THF at 60 °C furnished the corresponding bis (phosphine) containing cationic copper(I) and silver(I) complexes **3** and **4a/4b** in 89%, 88%, and 86% isolated yields, respectively, as off-white solids. It should be noted that 1:1 reactions of ligand and metal precursors also yielded the same complexes. The copper complexes **2** and **3** were found to be stable toward moisture and air; however, in the case of silver complexes, signs of decomposition were observed especially when exposed to light. **2–4** are highly soluble in polar solvents
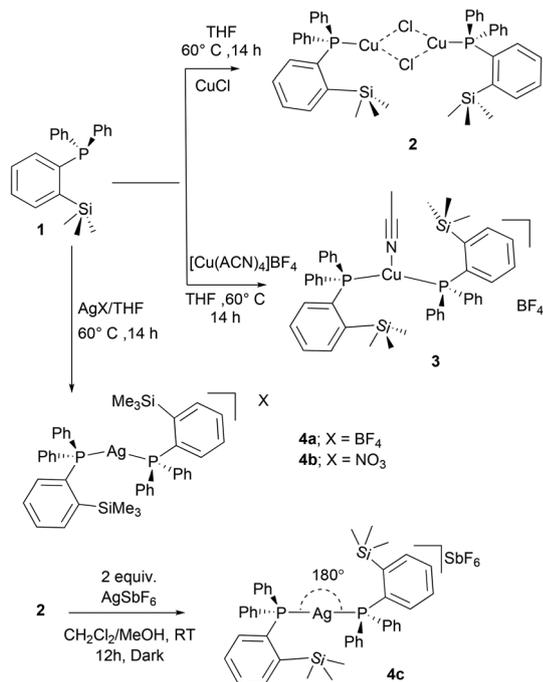
Scheme 2 Preparation of *ortho*-silylated phosphine-supported copper and silver complexes.

such as THF, CH_2Cl_2, and $CHCl_3$ but are insoluble in non-polar solvents. These complexes were fully characterized by spectroscopic techniques (^1H, ^{13}C, ^{31}P NMR, and MS) and by single crystal X-ray diffraction analysis.

The ^1H NMR spectra of **2–4** in $CDCl_3$ show the presence of trimethyl silyl groups as sharp and intense signals in the range of 0.28–0.38 ppm. The corresponding ^{13}C NMR spectrum of **3** displays a doublet at 2.05 ($^4J_{PC}$ = 2.8 Hz) ppm, whereas in the case of cationic **4a** (2.67 ppm) and **4b** (2.72, $^4J_{PC}$ = 3.9 Hz), broad doublets were observed. These chemical shifts are downfield shifted when compared with those of the free ligand (doublet at 1.6 ppm, $^4J_{PC}$ = 9.0 Hz).[10] Two sharp signals at 2.4 and 117.8 ppm in the ^{13}C NMR spectrum of **3** indicate the presence of the CH_3CN ligand attached to the copper center. The $^{31}P\{^1H\}$ NMR spectral data clearly indicate the coordination of the phosphine ligand to Cu and Ag metals. The copper complexes **2** (2.02 ppm) and **3** (0.29 ppm) show broad signals, which are significantly downfield shifted when compared to those of the free phosphine (−10.24 ppm) (**1**).[10] The broadening of these signals can be ascribed to the coupling of the ^{31}P nucleus with the quadrupole relaxation of ^{63}Cu and ^{65}Cu nuclei.[19] The signals observed at m/z 438.0845 (ESI Fig. S11/21†) in the ESI-MS spectral analysis of **2** and **3** could be assigned to the cationic species $[(1)Cu(CH_3CN)]^+$.

In comparison, the $^{31}P\{^1H\}$ NMR spectra of the cationic silver (I) complexes **4a/4b** in $CDCl_3$ show the silver-phosphorus couplings at RT (ESI; Fig. S23/31†). Complex **4a** exhibits a doublet resonance at δ = 13.3 ppm due to coupling with two silver isotopes ^{107}Ag (d, $^2J_{P,Ag(107)}$ = 746 Hz) and ^{109}Ag (d, $^2J_{P,Ag(109)}$ = 848 Hz), which are in the range reported for aminophosphine ligand-sup-

ported cationic silver complexes of the type $[Ag(PR)_3]BF_4$ (R = NMe_2, $NMeCH_2CMe$); (J_{AgP} = 811 and 910 Hz).[20,21] Similarly, **4b** with the NO_3^- anion shows a doublet at 13.9 ppm with slightly lower coupling constants with ^{107}Ag (d, $^2J_{P,Ag(107)}$ = 714) and ^{109}Ag (d, $^2J_{P,Ag(109)}$ = 821) isotopes (Fig. S31†). It can be observed that these coupling constants are significantly higher than those reported for two-coordinated phosphine-silver complexes,[20–22] and also considerably higher than those of the phosphorus(I) ligand-supported silver(I) complexes.[23]

In addition, we aimed to convert the dimeric copper(I) complex $[(1)CuCl]_2$ (**2**) to the corresponding cationic complex by chloride abstraction reactions. However, the reaction of **2** with $AgSbF_6$ in $MeOH/CH_2Cl_2$ mixture readily afforded another dicoordinate cationic silver(I) complex **4c** in 81% isolated yield as an off-white solid (Scheme 2). Similar to **4a/4b**, a doublet resonance in ^{31}P NMR (in $CDCl_3$) of **4c** at 12.4 ppm indicates the silver metal coordination. Interestingly, compared to the other silver complexes, significantly lower Ag–P coupling constants (d, $^2J_{P,Ag(107)}$ = 510 Hz, and $^2J_{P,Ag(109)}$ = 586 Hz) were observed as in the case of bis(phosphine)silver complexes.[24] This difference in coupling constants can be attributed to the presence of different weakly coordinating anions in **4a–4c**. In contrast to **2** and **3**, the ESI-MS spectral data clearly indicated the cationic nature of complexes **4a–4c**, and the m/z values at 777.1696 can be attributed to the cationic moieties of the type $[(1)_2Ag]^+$ (ESI, Fig. S28/33/37/39†). Additionally, the anionic SbF_6^- of **4c** was also detected at m/z 234.8944.

X-ray structural characterization of complexes 2–4

The solid-state molecular structures of **2–4** could be established by the single-crystal X-ray diffraction analysis. Single crystals suitable for the XRD measurements of copper complexes **2** (Fig. 2) and **3** (Fig. 3) were obtained by the vapor diffusion method by using the CH_2Cl_2/n-hexane combination. The complex **2** displays a dimeric structure in the solid state with an *ortho*-silylated phosphine-supported $Cu_2(\mu_2$-Cl)$_2$ core with a $Cu\cdots Cu$ separation of 3.00 Å.[25] It can be observed that
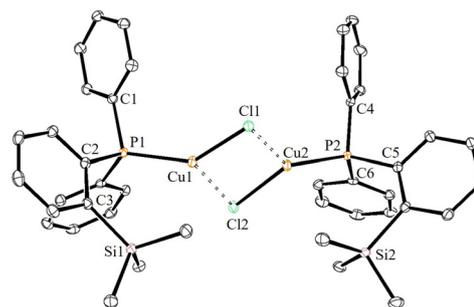
Fig. 2 ORTEP view of complex **2** with thermal displacement parameters drawn at 30% probability. Hydrogen atoms are omitted for clarity. Important bond lengths [Å] and angles [°]: P1–Cu1 2.1867(4), P2–Cu2 2.1759(4), Cu1–Cl1 2.3089 (4), Cu1–Cl2 2.3135 (5), Cu2–Cl2 2.2867 (4), Cu2–Cl1 2.3056 (4), Cu1–Cl1–Cu2 81.320(15), Cu1–Cl2–Cu2 81.625 (15), Cl1–Cu1–Cl2 97.294(16), Cl1–Cu2–Cl2 98.151(16), P1–Cu1–Cl1135.184(18), P1–Cu1–Cl2 127.086(18), P2–Cu2–Cl1 131.683(18), and P2–Cu2–Cl2 128.684(19).
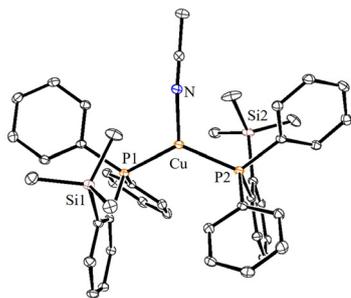
Fig. 3 ORTEP view of the cationic part of complex **3** with 30% ellipsoid probability. The BF_4^- counter anionic moiety and hydrogen atoms are omitted for clarity. Important bond lengths [Å] and angles [°]: P1–Cu 2.2694(5), P2–Cu 2.2681(5), Cu–N 1.9910(17), P1–Cu–P2 127.66(2), N–Cu–P1 118.26(5), and N–Cu–P2 113.99(5).

simple triphenyl phosphine–CuCl attains a cubane structure in the solid state having tetrameric $[PPh_3CuCl]_4$ nature with long Cu⋯Cu distances.[26] In contrast to this structure, complex **2** attains a dimeric nature in the solid state presumably due to the presence of a sterically bulky silyl group in the phosphine moiety, whereas the cationic complex **3** shows the formation of a tri-coordinate copper complex with two phosphine ligands and one acetonitrile coordination. The copper atom in **3** exhibits a distorted trigonal planar geometry with an average bond angle of 119.9° around the copper centre. The copper–phosphorus distances in **2** (av. 2.181 Å) are considerably shorter than those in **3** (av. 2.268 Å) due to the cationic nature of the complex. The dihedral angles between the two Cl–Cu–Cl in **2** are 97.28° (Cl1–Cu1–Cl2) and 98.15° (Cl1–Cu2–Cl2), which are consistent with the values reported in similar chloro-bridged copper complexes.[25]

The silver complexes **4a–4c** were also structurally characterized. Single crystals suitable for XRD analysis were grown by the vapor diffusion of dichloromethane solutions with *n*-hexane, and colorless crystals were used for the measurements. Their molecular structures are given in Fig. 4,
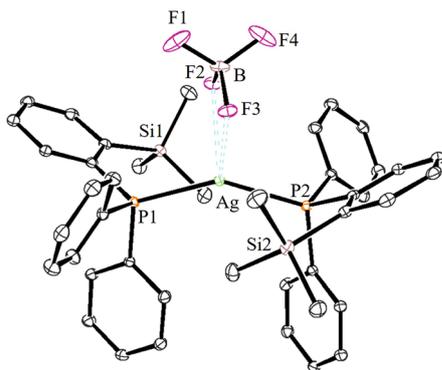
Fig. 4 ORTEP view of **4a** with thermal displacement parameters drawn at 30% probability. Hydrogen atoms are omitted for clarity. Important bond lengths [Å] and angles [°]: P1–Ag1 2.4241(5), P2–Ag1 2.4223(5), B1–F1 1.366(3), B1–F2 1.404(3), B1–F3 1.409(3), B1–F4 1.368(3), Ag1–F2 2.644, Ag1–F3 2.626, P1–Ag1–P2 147.34(2), and F3–Ag–F2 50.91.
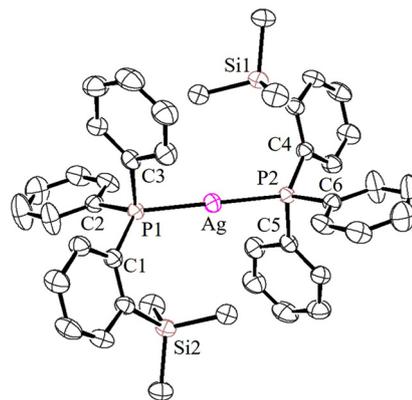
Fig. 5 ORTEP view of the cationic part of **4c** with thermal displacement parameters drawn at 30% probability. Counter anions and hydrogen atoms are omitted for clarity. Important bond lengths [Å] and angles [°]: P1–Ag 2.3936(6), P2–Ag 2.3936(6), and P1–Ag–P2 180.0 (exact linear unit).

Fig. S165† and Fig. 5, respectively. Although **4a–4c** contain the same phosphine **1**, the geometrical environment around the cationic silver(I) atoms is different. The average silver–phosphorus bond lengths in **4a** (2.423 Å) and **4b** (2.431 Å) are relatively longer than those observed in **4c** (2.393 Å); however, they are slightly shorter than those of similar tertiary phosphines that feature cationic silver complexes, for instance, $[(Mes_3P)_2Ag]BF_4$ (2.4409(9) Å),[27] but are comparable to those found for several other bis(phosphine)silver complexes.[28]

The P–Ag–P bond angles in **4a** (147.34(2)°) and **4b** (143.85(3)°) are far from linearity; however, complex **4c** with the SbF_6^- counter anion clearly exhibits a perfectly linear geometry with the P–Ag–P bond angle of 180.0°. This can be attributed to the interaction of anions with the Ag(I) centre in the case of **4a**/**4b**. It is noteworthy that, in general, bis(phosphine)silver complexes exhibit an almost linear geometry as reported in numerous previously reported examples.[27–29] Therefore, complex **4c** can be considered as one of the few bis(phosphine) supported dicoordinate silver complexes with a perfect linear P–Ag–P unit.

Furthermore, in contrast to **4c**, complexes **4a** and **4b** show weak interactions between the counter anions (BF_4^- and NO_3^-) and the cationic Ag(I) center. All the B–F bond distances in the tetrahedral BF_4 unit are different (free B–F bonds; 1.367 Å), and two of the B–F bonds show slightly elongated (B–F; av 1.406 Å) distances due to the weak ligating property toward the Ag(I) center. The observed average F⋯Ag distances (2.635 Å) in **4a** are shorter than those in BF_4-containing coordination polymers such as $\{[Ag(1,4\text{-}dithiane)]BF_4\}_∞$ (F⋯Ag; 2.886(2)).[30] Similarly, complex **4b** displays weak *O*, *O*-chelation of the NO_3^- anion with the Ag(I) center (Fig. S165†).

Reactivity of 1 with elemental sulfur, selenium, and their cationic homoleptic copper(I) complexes

In addition to the aforementioned class of *ortho*-silylated phosphine-containing cationic copper and silver complexes, we

have also isolated *ortho*-silylated phosphorus(v) compounds and investigated their reactivity toward [Cu(CH₃CN)₄]BF₄.

The treatment of **1** with elemental sulfur (S₈) and selenium (Se) powders in benzene at 50 °C readily afforded the corresponding phosphorus(v) compounds **5a** and **5b** in 88% and 93% isolated yields, respectively (Scheme 3). These compounds are highly soluble in both polar and nonpolar solvents. Their formation was further confirmed by ^{1}H and ^{31}P NMR spectroscopy and mass spectral analysis. As expected, the ^{31}P NMR spectra (in CDCl₃) of **5a** (46.6 ppm) and **5b** (37.7 ppm) showed sharp singlet resonances, which are significantly downfield shifted when compared with those of the free ligand **1** (δ = −10.24 ppm). These shifts are slightly downfield shifted compared to the corresponding triphenylphosphine sulphide and selenides.[31] Furthermore, their formation was supported by ESI-HRMS data (Fig. S43/47†). The signal at 367.1111 of **5a** can be assigned to [M + H]⁺ (calcd for C₂₁H₂₄PSSi 367.1106); similarly, for **5b**, *m/z* at 415.0550 can be assigned to [M + H]⁺.

Furthermore, the reactions of **5a/5b** with [Cu(CH₃CN)₄]BF₄ in a 3 : 1 ratio in CH₂Cl₂ at RT cleanly furnished the corresponding homoleptic and mono-cationic tris(phosphinochalcogenide)copper complexes of the type [(**5a/5b**)₃Cu]BF₄ in 85% (**6a**) and 79% (**6b**) isolated yields as stable solids (Scheme 3). The complexes **6a/6b** are soluble in polar solvents such as THF, CH₂Cl₂, and CHCl₃ but are insoluble in nonpolar solvents. The ^{1}H NMR spectra of **6a/6b** in CDCl₃ showed considerably up-field shifted (in comparison with the free ligands) singlet signals at δ = 0.09 and δ = 0.06 ppm, which can be assigned to the SiMe₃ groups. The corresponding ^{13}C NMR chemical shifts observed at δ = 2.74 (**6a**) and 2.97 (**6b**) can be assigned to the CH₃ carbons. The ^{31}P NMR spectra of **6a** and **6b** showed sharp singlets at 46.3 and 34.5 ppm, respectively. Furthermore, the CHNS data support the predicted composition of these complexes consisting of three phosphine chalcogenide ligands.[32] Single crystals suitable for XRD measurements of **6a** were grown by the vapor diffusion method from
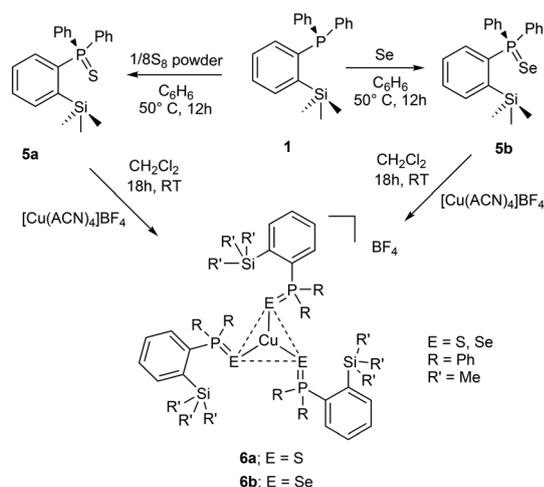
CH₂Cl₂ and *n*-hexane solution at RT. The molecular structure (Fig. 6) indicates the formation of a tri-coordinated and mono-cationic copper(ı) complex, with *C*3 symmetry in the molecule. The sum of the bond angles 119.42° and 106.93° corresponding to S–Cu–S and Cu–S–P, respectively, indicates the presence of a trigonal planar geometry around the copper center. Furthermore, the average copper–sulfur (S–Cu 2.254 Å) and phosphorus–sulfur bond distances (P–S 1.990 Å) fall in the range reported for three-coordinate copper(ı) complexes featuring tertiary phosphine sulfides.[32,33]

Catalytic studies of cationic copper(ı) complexes (2, 3 and 6a) in azide–alkyne cycloaddition reactions

To our knowledge, the transition metal complexes featuring ligands of type-**II** (Chart 1) in their mono-coordination fashion have rarely been explored in homogeneous catalysis as ancillary ligands. Recently, Si–H bond-containing type **II** (R′ = Me, R″ = H) phosphine ligand-supported metal complexes such as phosphinobenzylsilane–ruthenium,[34] iron,[13,14] cobalt,[4,35] rhodium,[36] and iridium[17] have been employed as molecular catalysts in various organic transformations. With this motivation and the newly synthesized copper(ı) complexes in hand, we chose to study the catalytic performance of [(**1**)CuCl]₂ (**2**), [(**1**)₂Cu(CH₃CN)]BF₄ (**3**) and [(**5a**)₃Cu]BF₄ (**6a**) in azide–alkyne cycloaddition reactions.[37,38] We first tested a series of reactions under various experimental conditions, such as by employing different solvents (CH₃CN, and CH₂Cl₂), temperatures, and catalyst loadings together with various other commercially available copper(ı) complexes (Table 1).
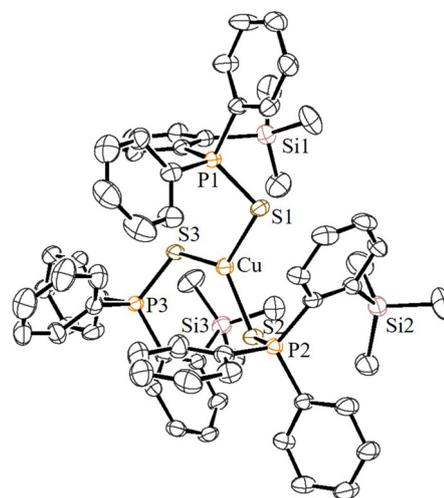
Fig. 6 ORTEP view of the cationic part of **6a** with thermal displacement parameters drawn at 30% probability. Hydrogen atoms are omitted for clarity. Important bond lengths [Å] and angles [°]: P1–S1 1.990(2), P2–S2 1.990(2), P3–S3 1.990(2), S1–Cu 2.2538(17), S2–Cu 2.2538(17), S3–Cu 2.2538(17), P1–Si1 3.690, P2–Si2 3.690, P3–Si3 3.690, S1–Si1 3.752, S2–Si2 3.752, S3–Si3 3.752, P1–S1–Cu 106.92(10), P2–S2–Cu 106.92(10), P3–S3–Cu 106.92(10), S1–Cu–S2 119.42(2), S2–Cu–S3 119.42(2), and S3–Cu–S1 119.42(2).

Scheme 3 Preparation of *ortho*-silylated phosphinochalcogenides and their cationic copper(ı) complexes (ACN = CH₃CN).

Table 1 Optimization of triazole synthesis using catalyst 3[a,b]
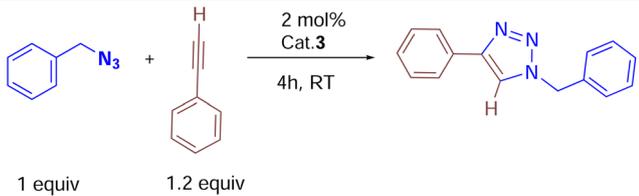
Entry	Deviation from the standard conditions yield of product[b] (%)	
1	None	99
2	Dichloromethane as reaction solvent	85
3	MeCN as a reaction solvent	79
4	1 mol% cat. **3**	89
5	0.5 mol% cat. **3**	81
6	Alkyne 1 equiv.	90
7	Alkyne 1.5 equiv	98
8	2 mol% complex **2**	89
9	2 mol% (PPh₃)CuCl as catalyst	88
10	2 mol% CuCl	70
11	2 mol% CuI	79

[a] Reaction conditions: azide (0.1 mmol), alkyne (0.12 mmol), cat. **3** (2 mol%), neat conditions, RT, 4 h. [b] isolated yields.

We began by screening **2** and **3** for their ability to synthesize various triazoles. Under neat solvent-free conditions (entry 1), the reaction of benzyl azide with phenyl acetylene and 2 mol% **3** at room temperature produced the corresponding triazole **7k** in a 99% isolated yield (Table 2), while lower catalyst loadings

(entry 5; 0.5 mol%) showed lower yields. Furthermore, catalyst **3** showed better conversion rates (99% entry **1**) within 4 h than the neutral complex **2** (89%, entry **8**), showing the superiority of cationic complex **3** over the neutral complex **2**. In addition, under the same optimized experimental conditions, we screened other commercially available copper(I) halides by keeping complex **3** as the reference. For instance, as shown in entries 10 and 11, ligand-free copper halides furnished moderate yields; however, [Ph₃PCuCl] gave relatively higher yields, indicating the requirement of ligand-supported cationic copper systems (Table 1). The polar solvents like CH₃CN and CH₂Cl₂ provided good yields, but the majority of the reactions furnished excellent yields under solvent-free conditions. It should be noted that based on the physical state of substrates, in some cases, (carbazolyl triazole as well as bis-triazole derivatives) dichloromethane was employed as the reaction medium.

Under the optimized conditions, a series of three different classes of triazole derivatives (7, Table 2; 8 and 9, Table 3) were obtained. The first set of triazoles **7a–7r** was achieved in 70–99% isolated yields. In the second set of five triazoles, **8a–8e**[39] bearing alkyl-phenyl propargylic ether groups were prepared by employing a series of azides (benzyl azide, tolylazide, and carbazolyl azides) and terminal-internal alkynes as coupling partners (Table 3). It should be noted that, triazoles **8a–8d** are yellow viscous compounds, whereas **8e** is solid in nature at room temperature. The molecular compositions of triazole derivatives **8** were assigned by ¹H, ¹³C NMR, and HRMS analysis (Fig. S129–145†). The presence of propargylic ether groups in triazoles **8** could be observed in the range of chemi-

Table 2 Substrate scope of various triazoles synthesized using catalyst 3

Table 3 Substrate scope of various triazoles bearing alkyne-phenylpropargylic ether substituents and bis-triazoles
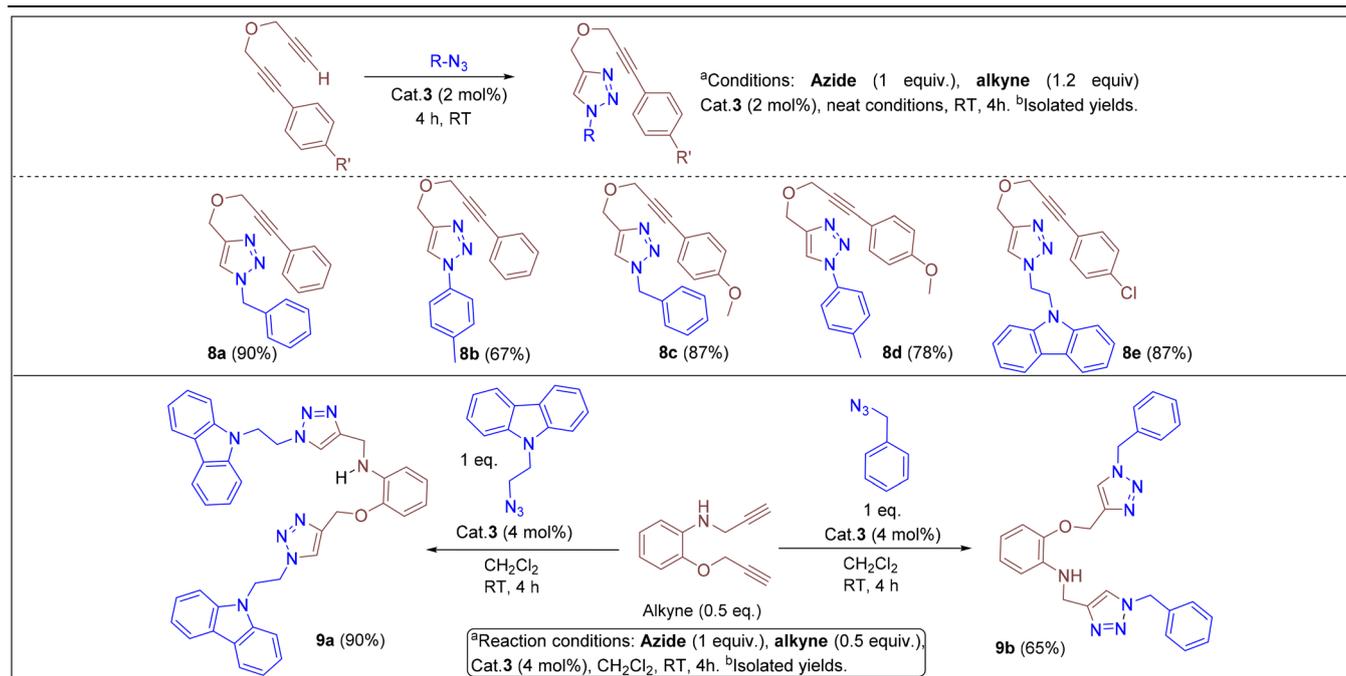
cal shifts δ = 83–89 ppm in their ^{13}C NMR spectra (in CDCl$_3$) in addition to their aromatic carbons. Additionally, the solid-state molecular structure of the triazole **8e** was established. Single crystals suitable for XRD measurements were grown by slow evaporation of the dichloromethane solution at RT. Compound **8e** crystallizes in the monoclinic system, and its structure clearly displays the presence of carbazolyl and phenyl propargylic ether groups at the 1 and 4-positions of the triazole (Fig. 7).

In addition, we tested the catalytic performance of **3** in the cyclization reactions of bis(terminal)alkyne with carbazolyl and benzyl azides (Table 3). Starting from the bis-alkyne, the new bis-triazoles **9a** (90%) and **9b** (65%) could be selectively

achieved by employing 4 mol% catalyst loadings in dichloromethane at room temperature. The 1 : 2 reaction of bis(alkyne) and carbazolyl azide in the presence of 4 mol% catalyst showed a brown precipitate formation within 10 min; this precipitate further turned into a viscous yellow substance. Washing with CH$_2$Cl$_2$ yielded **9a** as a pale-brown solid in 90% isolated yield without any further purification steps. Interestingly, **9a** could also be obtained in 77% isolated yield within 10 min, indicating the efficient catalytic performance of **3** (Scheme S4†); however, for achieving further higher yields, it was stirred for 4 h. **9a** was insoluble in CH$_2$Cl$_2$ and CHCl$_3$, but had minimal solubility in ethanol and methanol. **9a** was fully characterized by ^{1}H and ^{13}C NMR and by HMRS analytical data. A signal at m/z = 658.3066 in the HRMS spectrum can be assigned to [M + H]$^+$ calcd for 658.3043 (C$_{40}$H$_{36}$N$_9$O).

We have also examined the catalytic efficiency of silyl-phosphine sulfide ligand (**5a**) supported cationic complex **6a** in the azide–alkyne cycloaddition reactions. Interestingly, 2 mol% catalyst loading of [(**5a**)$_3$Cu]BF$_4$ can also catalyze the cycloaddition of benzyl azide with phenylacetylene; by this reaction, we could achieve triazole **7k** in 92% isolated yield as a clean product (Scheme S6, and Fig. S155†). This reaction shows the potential applications of silyl group-functionalized phosphine sulfide systems as ancillary ligands in homogeneous catalysis. For a detailed understanding of the reaction mechanism, a series of supporting experiments (Scheme S1–3†) were performed. As shown in Fig. S64,† the 1 : 1 : 1 reaction of benzyl azide, phenylacetylene, and cat. **3** in an NMR tube clearly showed the progression of the reaction toward the anticipated cyclization reaction to give the triazole
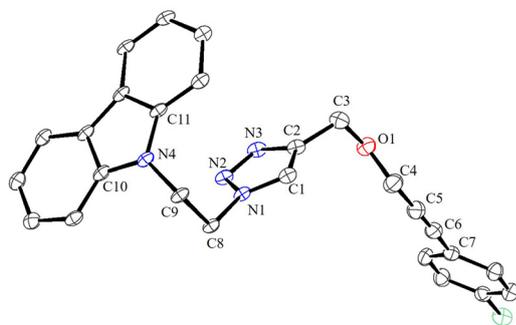
Fig. 7 ORTEP view of **8e** with thermal displacement parameters drawn at 30% probability. Hydrogen atoms are omitted for clarity. Important bond lengths [Å] and bond angles [°]: N1−C1 1.448 (4), C1−C2 1.528 (4), C2−N2 1.457 (4), O−C5 1.429 (4), O−C6 1.417 (5), and C6−C7 1.456 (6).

Paper

derivative. In the presence of cat. **3**, the **a** and **b** (Scheme S3†) protons of the corresponding azide and phenyl acetylenes vanish during the course of the reaction to selectively afford triazole **7k** with complete conversion. Noteworthily, the catalytic efficiency of the reported complex is comparable to that of a series of other phosphine,[40] phosphinite and phosphonite[41] ligand-supported copper(I) systems; however, with cat. **3**, triazoles consisting of internal alkyne groups could be achieved selectively.

For further understanding of the homogeneity of the catalytic reaction with cat. **3**, we have performed a series of mercury drop experiments (Scheme S7†) in 2 : 150 mol% of cat. **3** to Hg metal. Four different substrates were screened, and no significant changes in the overall isolated yields were observed, which indicates the homogeneous pathway of the reported catalytic cycle.

Azide–alkyne cycloaddition reactions catalysed by copper(I) catalysts have been widely studied, and numerous studies extensively investigated their mechanistic pathways both by theoretical and experimental methods.[38,42,43] Accordingly, a plausible mechanism could be derived as depicted in Fig. 8. The bis(phosphine) copper complex **3** would be transformed into acetylide **A** by releasing one phosphine ligand, which then coordinates with azide to form intermediate **B**. It could then further rearrange to a six-membered metallacycle intermediate **C**.[44] Intermediate **C** can further rearrange to form *ortho*-silylated phosphine containing copper(I) triazolide intermediate **D**. Furthermore, proteolysis of **D** releases the corresponding triazole product by regenerating the catalyst. For further detection of intermediate **C**, two reactions with different substrates were performed, and they were analysed by the *in situ* ESI-MS technique at different intervals of the reaction course.
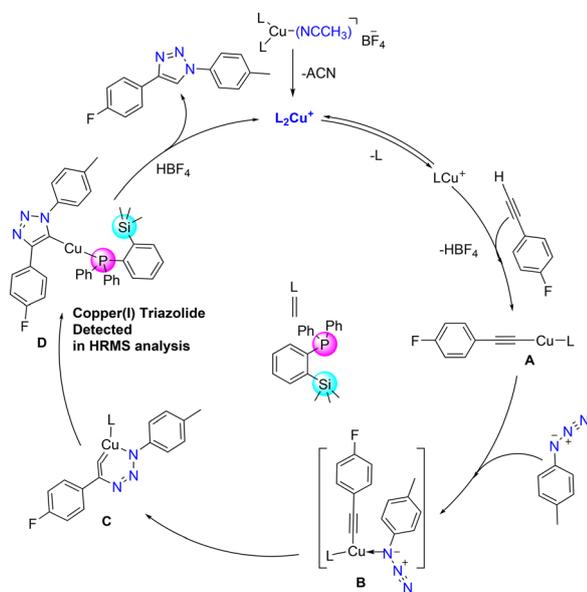
The HRMS spectrum showed the presence of the copper(I) triazolide intermediate [(triazolide)Cu(**1**)] consisting of the *meso*-ionic carbene[45,46] and the phosphine **1** as shown in Fig. S62† (exp. 650.1650 [M + H]$^+$, calcd 650.1618 for $C_{36}H_{35}CuFN_3PSi$) and Fig. S63† (exp. 632.1751 [M + H]$^+$, calcd 632.1712 for $C_{36}H_{36}CuN_3PSi$). Several attempts to isolate these intermediates resulted in the formation of the corresponding triazoles, indicating their highly reactive nature. It should be noted that Straub and co-workers isolated heteroleptic copper(I)triazolide (click intermediate) for the first time and also established its molecular structure.[43,46] In addition to the above catalytic reactions by conventional methods, cat. **3** was also employed in the mechanical grinding method using 2 mol% catalyst loading (Scheme S5†). Under solvent-free conditions, azide/alkyne/catalysts were mixed and mortared for 5 min for the isolation of pure triazole **7k** in 86% yield (Fig. S67†).

Conclusions

In summary, a series of neutral and mono-cationic complexes of copper(I) and silver(I) bearing a sterically bulky diphenyl(2-(trimethylsilyl)phenyl)phosphine ligand were synthesized in excellent yields and structurally characterized. In the case of silver complexes, the solid-state molecular structures show the presence of linear and nonlinear P–M–P (M = Ag) units depending on the counter anions and their interaction with the cationic central metal atoms. The *ortho*-silylated phosphine was conveniently converted to its sulfide and selenides, and their cationic homoleptic copper(I) complexes of the type [(**5a/5b**)$_3$Cu]BF$_4$ were isolated. The latter phosphine sulfide complex displayed a trigonal planar environment around the tricoordinate copper center.

The catalytic performance of **2**, **3** and **6a** was tested in the azide–alkyne cycloaddition reactions (CuAAC); among them, complex **3** displayed high catalytic activity for the preparation of three sets of triazoles which were achieved in good to excellent yields under very mild conditions. Cat. **3** displayed high selectivity towards terminal alkynes over internal alkyne groups. The present work showed the formation of the click intermediate [(triazolide)Cu(phosphine)], indicating the presence of silylated phosphine-bound copper species during the catalytic reaction. Overall, the *ortho*-silylated phosphine and its sulfide derivatives were first time introduced as potential ancillary ligands in homogeneous catalysis.

Experimental section

Materials and methods

All the reactions were performed under a strictly dry argon/nitrogen atmosphere using the standard Schlenk line technique. Freshly distilled solvents (CH$_3$CN, THF, CH$_2$Cl$_2$, n-hexane, diethyl ether, and ethylacetate) were used for the reactions reported in this study. All the chemical shifts are

Fig. 8 Proposed reaction mechanism for the formation of 1,4-substituted triazole derivatives catalyzed by cat. **3**.

reported in ppm and spectra are referenced to the corresponding residual solvent peaks. Elemental analysis was measured on an Elimentar instrument. The NMR spectra (^{1}H, ^{13}C, ^{31}P, ^{19}F, and ^{11}B NMR) were obtained using Bruker Avance 400 and 700 MHz NMR spectrometers. The ESI mass spectral data were measured using a Waters Xevo G2-XS QTof instrument in CH_3OH or CH_3CN solvents. The required compound $[Cu(CH_3CN)_4]BF_4$ was purchased from commercial sources. The phosphine-copper complex $ClCu(PPh_3)$ was prepared according to a reported procedure.[47]

Crystallography

Single crystals of **1–3**, **4a**, **4b**, **4c**, **6a** and **8e** were mounted on a nylon loop under a microscope using a paraffin bar, and X-ray data were collected on the Rigaku Super Nova fine-focused dual diffractometer, with CuKα radiation ($\lambda = 1.54178$ Å) and MoKα radiation (0.71073 Å) equipped with a PILATUS200K. Using Olex2, the structures were solved with the SHELXS structure solution program using direct methods and refined with the SHELXL refinement package. The CCDC numbers of the compounds reported in this study are: 2264786 (**1**), 2264791 (**2**), 2264787 (**3**), 2264784 (**4a**), 2264789 (**4b**), 2264788 (**4c**), 2264785 (**6a**), and 2264790 (**8e**).†

Synthesis of the reported compounds 1–9

Preparation of *ortho*-silylated phosphine (1). A slightly modified method was used from the procedure reported previously.[10] A 50 mL well-dried Schlenk flask was charged with the bromophosphine {o-PPh$_2$(C$_6$H$_4$)Br} (200 mg, 0.586 mmol, 1 equiv.) in diethyl ether (25 mL), and the reaction mixture was cooled to 0 °C. To this cold solution was slowly added 0.44 mL of *n*-BuLi (2.0M in cyclohexane, 1.5 equiv.). Then, the reaction mixture was kept at 0 °C for 20 min, and after that, ClSi(CH$_3$)$_3$ (0.15 mL, 1.172 mmol, 2 equi.) was added to the reaction mixture at the same temperature. The resulting reaction mixture was warmed to room temperature gradually and stirred for an additional 14 h at RT. After removing the volatiles under vacuum, the resulting residue was dissolved in ether (10 mL) and purified by column chromatography using a silica gel column (7 cm). Elution with *n*-hexane (250 mL) and evaporation of the solvent under vacuum afforded a colorless oily substance. Yield: 82.7% (162 mg). ^{1}H NMR (400 MHz, CDCl$_3$): δ = 7.67–7.60 (m, 1H), 7.37–7.27 (m, 8H), 7.25–7.19 (m, 4H), 7.17 (dd, J = 7.0, 4.0 Hz, 1H), and 0.38 (d, J = 1.3 Hz, 9H). ^{13}C NMR (101 MHz, CDCl$_3$): δ = 143.5–142.9 (m), 138.7–137.9 (m), 135.4, 135.3–134.3 (m), 133.4 (d, J = 18.6 Hz), 129.3, 128.5 (d, J = 6.4 Hz), 128.3, and 1.5 (d, J = 9.5 Hz). ^{31}P{^{1}H} NMR (162 MHz, CDCl$_3$): δ = −10.24 (s). Analytical data for (C$_{21}$H$_{23}$PSi): calcd (%): C, 75.41; H, 6.93; found: C, 75.53; H, 6.943.

Preparation of [(1)CuCl]$_2$ (2). To a 50 mL Schlenk tube containing diphenyl(2-(trimethylsilyl)phenyl)phosphine (**1**) (75 mg, 0.224 mmol) and CuCl (22.20 mg, 0.224 mmol) was added freshly distilled dry THF (7 mL), and the resulting reaction mixture was stirred at 60 °C for 14 h. After 2 h of heating a white suspension was observed. The reaction mixture was fil-

tered to remove unreacted CuCl, and the solvent was removed under vacuum. The resulting pale-yellow solid was washed with *n*-hexane (3 × 5 mL) and dried under vacuum to afford **2** as a white powder. Yield: 86 mg (87.5%). ^{1}H NMR (400 MHz, CDCl$_3$): δ = 7.73 (d, J = 6.4 Hz, 1H, ArH), 7.41 (s, 10H, ArH), 7.26 (s, 2H, Ar H), 6.88 (s, 1H, ArH), and 0.38 (s, 9H, SiMe$_3$). ^{31}P NMR (162 MHz, CDCl$_3$): δ = 2.02 (br). ^{13}C NMR (176 MHz, CDCl$_3$): δ = 146.2 (d, J = 28.3 Hz), 136.6 (d, J = 14.8 Hz), 134.5 (d, J = 14.4 Hz), 134.1 (s), 132.3 (d, J = 9.9 Hz), 130.6 (s), 129.4 (s), 129.1 (d, J = 9.8 Hz), 128.5 (d, J = 12.3 Hz), and 2.70 (SiMe$_3$) (s). (HRMS, CH$_3$CN, *m/z*): [M$^+$] calcd for C$_{23}$H$_{26}$CuNPSi: 438.0845; calcd for 438.0868 (M−Cl + CH$_3$CN)$^+$; analytical data for (C$_{42}$H$_{46}$Cl$_2$Cu$_2$P$_2$Si$_2$): calcd (%): C 58.19; H 5.35; found: C 59.70; H 5.740.

Preparation of [(1)$_2$Cu(CH$_3$CN)]BF$_4$ (3). To a 50 mL Schlenk tube was added diphenyl(2-(trimethylsilyl)phenyl)phosphine (90 mg, 0.27 mmol) and [Cu(CH$_3$CN)$_4$]BF$_4$ (42.3 mg, 0.135 mmol). To this solid mixture, 10 mL of dry THF was added, and the resulting colourless reaction mixture was heated at 60 °C for 14 h. After 2 h of stirring a light yellow suspension was observed as in the case of **2**. The solvent was removed under reduced pressure, the resulting pale-yellow solid was washed with *n*-hexane (3 × 7 mL), and then it was dried under high vacuum to afford **3** as a white solid. Yield: 103.4 mg (89%). ^{1}H NMR (400 MHz, CDCl$_3$): δ = 7.74 (s, 1H, Ar H), 7.44 (s, 7H, Ar-H), 7.26 (s, 5H, Ar-H), 6.86 (s, 1H, ArH), 2.27 (s, 10H, CH$_3$CN), 0.28 (s, 9H, SiMe$_3$). ^{31}P NMR (162 MHz, CDCl$_3$): δ = 0.29 (s). ^{19}F NMR (377 MHz, CDCl$_3$): δ = −153.3 (s). ^{11}B NMR (128 MHz, CDCl$_3$): δ = −0.92 (s). ^{13}C NMR (101 MHz, CDCl$_3$): δ = 145.9–144.9 (m), 136.8 (d, J = 14.9 Hz), 136.1–135.4 (m), 133.9 (d, J = 14.7 Hz), 131.3 (d, J = 39.9 Hz), 129.8–129.0 (m), 117.8 (s, CH$_3$*C*N), 2.4 (s, *C*H$_3$CN), and 2.0 (d, J = 2.8 Hz, Si*Me*$_3$). Mass spectral data (HRMS, CH$_3$CN, *m/z*): [M$^+$] calcd for C$_{23}$H$_{26}$CuNPSi: 438.0886 calcd for 438.0868 (M−phosphine)$^+$; found. Analytical data for (C$_{44}$H$_{49}$BCuF$_4$NP$_2$Si$_2$): calcd (%): C 61.43; H 5.74; N 1.63 found: C 60.9; H 5.527; and N 1.58.

Preparation of [(1)$_2$Ag]BF$_4$ (4a). Freshly distilled THF (10 mL) was added to a Schlenk tube containing diphenyl(2-(trimethylsilyl)phenyl)phosphine (94 mg, 0.28 mmol) and AgBF$_4$ (27.4 mg, 0.14 mmol). The colorless reaction mixture was heated at 60 °C for 14 h, after which it was filtered and the solvent was removed under vacuum. The resulting white solid was washed with *n*-hexane (3 × 5 mL), and dried to afford the silver complex. Yield: 106.4 mg (88%). ^{1}H NMR (400 MHz, CDCl$_3$): δ = 7.77 (d, J = 7.2 Hz, 1H, ArH), 7.45 (m, J = 7.0 Hz, 8H), 7.32 (m, J = 17.3, 7.3 Hz, 4H), 6.91 (m, 1H, ArH), 0.31 (s, 9H, SiMe$_3$). ^{31}P NMR (162 MHz, CDCl$_3$): δ = 13.3 (dd, $^2J_{P,Ag(107)}$ = 746 Hz) and ($^2J_{P,Ag(109)}$ = 848 Hz). ^{11}B NMR (128 MHz, CDCl$_3$): δ = −0.9 (s). ^{19}F NMR (377 MHz, CDCl$_3$): δ = −150.6 (s). ^{13}C NMR (101 MHz, CDCl$_3$): δ = 145.9 (d, J_{pc} = 29.4 Hz), 137.1 (d, J_{pc} = 12.9 Hz), 134.5 (d, J_{pc} = 14.3 Hz), 131.6 (s), 130.3 (s), 129.7 (s), and 2.7 (s, SiMe$_3$). Mass spectral data (HRMS, CH$_3$CN, *m/z*): [M$^+$] calcd for C$_{42}$H$_{46}$AgP$_2$Si$_2$: 775.1664; found 775.1699 [(1)$_2$Ag]$^+$. Analytical data for (C$_{42}$H$_{46}$BAgF$_4$P$_2$Si$_2$): calcd (%): C, 58.41; H, 5.37 found: C, 57.00; H, 5.305.

Preparation of [(1)$_2$Ag]NO$_3$ (4b). Synthetic and work-up procedures are the same as those of complex **4a**; to a Schlenk tube containing **1** (110 mg, 0.33 mmol) and the silver salt AgNO$_3$ (28 mg, 0.16 mmol) was added 10 mL of dry THF, and the mixture was heated at 60 °C for 14 h. Off-white solid (*light sensitive*). Yield: 115.4 mg (86%). ^{1}H NMR (400 MHz, CDCl$_3$): δ = 7.79 (d, J = 3.4 Hz, 1H), 7.54–7.42 (m, 7H), 7.40–7.29 (m, 5H), 7.00–6.88 (m, 1H), 0.35 (s, 8H). ^{31}P NMR (162 MHz, CDCl$_3$): δ = 13.91 (dd, $^2J_{P,Ag(107)}$ = 714) and ($^2J_{P,Ag(109)}$ = 821). ^{13}C NMR (101 MHz, CDCl$_3$): δ = 146.2 (d, J = 29.0 Hz), 137.1 (d, J = 15.8 Hz), 134.9–133.6 (m), 131.6 (d, J = 2.0 Hz), 130.3 (dd, J = 21.9, 19.6 Hz), 129.7 (d, J = 10.9 Hz), 129.5 (d, J = 7.2 Hz), and 2.7 (d, J_{PC} = 3.9 Hz, SiMe$_3$). Mass spectral data (HRMS, CH$_3$CN, m/z): [M$^+$] calcd for C$_{42}$H$_{46}$AgP$_2$Si$_2$: 775.1664; found 775.1713 for [(phosphine)$_2$Ag]$^+$. Analytical data for (C$_{42}$H$_{46}$AgNO$_3$P$_2$Si$_2$): calcd (%): C 60.14; H 5.53; N 1.67 found: C 59.50; H 5.408; N 1.70.

Preparation of [(1)$_2$Ag]SbF$_6$ (4c). To a Schlenk tube containing **2** (25 mg, 0.029 mmol) in dry CH$_2$Cl$_2$ (7 mL), AgSbF$_6$ (21.7 mg, 0.063 mmol) in methanol (5 mL) was slowly added over a period of 2 min. The resulting brownish-grey reaction mixture was stirred at RT for 14 h. Then, this mixture was filtered and the filtrate part was dried under high vacuum, and the resulting solid was washed with diethyl ether (3 × 5 mL) and dried under vacuum to afford **4c**. Yield: 23.8 mg (81%). ^{1}H NMR (400 MHz, CDCl$_3$): δ = 7.78 (d, J = 7.1 Hz, 1H), 7.62–7.44 (m, 6H), 7.42–7.23 (m, 6H), 6.99 (m, 1H), and 0.19 (s, 9H). ^{31}P NMR (162 MHz, CDCl$_3$): δ = 12.4 (dd, $^2J_{P,Ag(107)}$ = 510 Hz, and $^2J_{P,Ag(109)}$ = 586 Hz). ^{13}C NMR (101 MHz, CDCl$_3$): δ = 137.3, 134.8, 134.1, 132.2, 130.9, 130.1, 128.9, and 2.8 (s, SiMe$_3$). Mass spectral data (HRMS, positive mode, CH$_3$CN, m/z): [M$^+$] calcd for C$_{42}$H$_{46}$AgP$_2$Si$_2$: 775.1664; found 775.1671 for [(phosphine)$_2$Ag]$^+$. HRMS (negative mode); found 234.8944; cacld 234.8942 for [SbF$_6$]$^-$. Analytical data for (C$_{42}$H$_{46}$SbAgF$_6$P$_2$Si$_2$): calcd (%): C 49.82; H 4.58; found: C 48.09; H 4.177.

Preparation of phosphine sulfide (5a). To a Schlenk tube containing phosphine (**1**) (67.2 mg, 0.201 mmol) and elemental sulfur powder (6.5 mg, 0.201 mmol) was added dry benzene (10 mL) (*caution: carcinogenic*); it was then heated to 50 °C overnight. The resulting reaction solution was filtered, the solvent was removed under reduced pressure, and then, it was dried under vacuum to afford **5a** as a faint-yellow solid. Yield: 65 mg (88%). ^{1}H NMR (400 MHz, CDCl$_3$): δ = 7.89 (s, 1H, ArH), 7.67 (dd, J = 7.6 Hz, 4H, ArH), 7.57–7.33 (m, 7H, ArH), 7.18 (s, 1H, ArH), 6.93 (dd, 1H, ArH), and 0.21 (s, 9H, SiMe$_3$). ^{31}P NMR (162 MHz, CDCl$_3$): δ = 46.6 (s). ^{13}C NMR (101 MHz, CDCl$_3$): δ = 146.3 (d, J_{PC} = 19.3 Hz), 139.3 (d, J_{PC} = 87.4 Hz), 138.1 (d, J_{PC} = 16.1 Hz), 134.8 (s), 133.9 (s), 133.4 (d, J_{PC} = 14.7 Hz), 132.7 (d, J_{PC} = 10.5 Hz), 131.5 (d, J_{PC} = 2.9 Hz), 130.2 (d, J_{PC} = 3.2 Hz), 128.6 (d, J_{PC} = 12.4 Hz), 127.8 (d, J_{PC} = 12.8 Hz), and 2.7 (s, SiMe$_3$). Mass spectral data (HRMS, CH$_3$CN, m/z): 367.1111; calcd 367.1106 for [M + H]$^+$.

Preparation of phosphine selenide (5b). **5b** was synthesized by the same method as that of **5a**; phosphine (**1**) (61 mg, 0.183 mmol) and Se powder (14.5 mg, 0.183 mmol) were taken

in a Schlenk tube, dry benzene (10 mL) was added and then, the mixture was heated to 50 °C overnight. It was then filtered, and the solvent was removed under vacuum to afford **5b** as an off-white solid. Yield: 71 mg (93%). ^{1}H NMR (400 MHz, CDCl$_3$): δ = 7.88 (s, 1H, ArH), 7.73 (dd, J = 7.5 Hz, 4H, ArH), 7.55–7.38 (m, 7H, ArH), 7.17 (t, J = 7.1 Hz, 1H, ArH), 6.87 (dd, J = 7.8 Hz, 1H, ArH), 0.20 (s, 9H, SiMe$_3$). ^{13}C NMR (101 MHz, CDCl$_3$): δ = 146.5 (d, J_{PC} = 12.0 Hz), 139.0 (s), 138.3 (d, J_{PC} = 16.3 Hz), 133.3 (d, J_{PC} = 10.6 Hz), 132.8 (d, J_{PC} = 47.5 Hz), 131.6 (d, J_{PC} = 3.0 Hz), 130.2 (s), 128.6 (d, J_{PC} = 12.4 Hz), 127.9 (d, J_{PC} = 12.4 Hz), and 2.9 (s, SiMe$_3$). ^{31}P {^{1}H} NMR (162 MHz, CDCl$_3$): δ = 37.7 (s). Mass spectral data (HRMS, CH$_3$CN, m/z): 415.0204; calcd for C$_{21}$H$_{24}$PSeSi: 415.0551 [M + H]$^+$. Analytical data for (C$_{21}$H$_{23}$PSeSi): calcd (%): C 61.01; H 5.61; found: C 61.42; H 5.439.

Preparation of [(5a)$_3$Cu]BF$_4$ (6a). To a 50 mL Schlenk tube were added **5a** (60 mg, 0.163 mmol) and [Cu(CH$_3$CN)$_4$]BF$_4$ (17.4 mg, 0.054 mmol). To this solid mixture was added dry CH$_2$Cl$_2$ (7 mL), and the resulting reaction solution was stirred for 18 h at RT. Then, it was filtered, and the solvent was removed under reduced pressure. The resulting substance was washed with *n*-hexane (3 × 5 mL) and then dried under vacuum to afford complex **6a** as an off-white solid. Yield: 57.4 mg (83%). ^{1}H NMR (400 MHz, CDCl$_3$): δ = 7.91 (s, 1H, ArH), 7.66–7.40 (m, 11H, ArH), 7.23 (s, 1H, ArH), 6.94 (dd, J = 7.7 Hz, 1H, ArH), 0.09 (s, 9H, SiMe$_3$). ^{31}P NMR (162 MHz, CDCl$_3$): δ = 46.3 (s). ^{13}C NMR (101 MHz, CDCl$_3$): δ = 146.4 (d, J_{PC} = 19.3 Hz), 138.5 (d, J_{PC} = 16.2 Hz), 134.3 (d, J_{PC} = 15.7 Hz), 132.8 (d, J_{PC} = 10.4 Hz), 132.6 (s), 131.2 (s), 129.0 (d, J_{PC} = 12.6 Hz), 128.2 (d, J_{PC} = 13.1 Hz), and 2.7 (s, SiMe$_3$). ^{11}B NMR (128 MHz, CDCl$_3$): δ = −0.96 (s). ^{19}F NMR (377 MHz, CDCl$_3$): δ = −153.5 (s). Mass spectral data (ESI-HRMS, CH$_3$CN, m/z): 470.0593; calcd for C$_{23}$H$_{26}$CuNPSSi: 470.0589 [Cu(phosphine sulfide)]$^+$. Analytical data for (C$_{63}$H$_{69}$BCuF$_4$P$_3$Si$_3$S$_3$)·CH$_2$Cl$_2$: calcd (%): C 57.54; H 5.36; S 7.69; found: C 57.42; H 5.321; S 7.531.

Preparation of [(5b)$_3$Cu]BF$_4$ (6b). Freshly dried CH$_2$Cl$_2$ was added to a Schlenk tube containing **5b** (65 mg, 0.157 mmol) and [Cu(CH$_3$CN)$_4$]BF$_4$ (14.4 mg, 0.047 mmol), and the resulting mixture was stirred for 18 h at RT. Then, it was filtered, and the solvent was removed under reduced pressure. The resulting substance was washed with *n*-hexane (2 × 4 mL) and then dried under vacuum to afford complex **6b** as an off-white solid. Yield: 51.7 mg (79%). H NMR (400 MHz, CDCl$_3$): δ = 7.95–7.84 (m, 1H, ArH), 7.59 (m, 7H, ArH), 7.53–7.40 (m, 4H, ArH), 7.21 (t, J = 7.0 Hz, 1H, ArH), 6.86 (dd, J = 7.8 Hz, 1H, ArH), 0.06 (s, 9H, SiMe$_3$). ^{31}P NMR (162 MHz, CDCl$_3$): δ = 34.5 (s). ^{13}C NMR (101 MHz, CDCl$_3$): δ = 146.7 (d, J_{PC} = 20.3 Hz), 138.8 (d, J_{PC} = 16.8 Hz), 134.3 (d, J_{PC} = 14.5 Hz), 133.4 (d, J_{PC} = 10.4 Hz), 133.1 (s), 132.98 (s), 131.3 (s), 130.0 (s), 129.2 (d, J_{PC} = 12.4 Hz), 128.5 (d, J_{PC} = 12.7 Hz), and 2.96 (s, SiMe$_3$). ^{11}B NMR (128 MHz, CDCl$_3$): δ = −0.95 (s). ^{19}F NMR (377 MHz, CDCl$_3$): δ = −153.5 (s). Mass spectral data (HRMS, CH$_3$CN, m/z): 891.0344; calcd for C$_{42}$H$_{46}$CuP$_2$Se$_2$Si$_2$: 891.0247 [Cu(SeP)$_2$]$^+$. Analytical data for C$_{63}$H$_{69}$BCuF$_4$P$_3$Si$_3$Se$_3$: calcd (%): C 54.41; H 5.00; found: C 54.42; H 5.324.

Catalytic reactions and general experimental procedures for substituted triazoles

Synthesis of 7a–7l, 7n, 7o, 7q, and 7r using catalyst 3. To a 25 mL Schlenk tube charged with a magnetic stirring bar was added the corresponding azide (1 equiv.), alkyne (1.2 equiv.) and cat. **3** (2 mol%) under a N$_2$ atmosphere. The reaction mixture was then stirred for 4 h at room temperature, and the crude mixture was purified by silica gel flash column chromatography using ethyl acetate as an eluent. The substances obtained were washed with *n*-hexane followed by drying under a vacuum to afford the corresponding triazoles as solid products. The spectral data (^{1}H, ^{13}C, and HRMS) of all these products are given in the ESI.† The corresponding citations are given to those already reported in the literature.

Synthesis of triazoles 7m and 7p using catalyst 3. To a Schlenk tube containing the corresponding azide (1 equiv.), alkyne (1.2 equiv.) and cat. **3** (2 mol%), CH$_2$Cl$_2$ (1 mL) was added under a N$_2$ atmosphere. The resulting colorless reaction mixture was stirred for 4 h at RT, during which the formation of white precipitate was observed. It was then filtered and washed with dichloromethane (3 × 5 mL), followed by *n*-hexane (2 × 3 mL), to afford off-white solids. The spectral data (^{1}H, ^{13}C, and HRMS) of **7m** and **7p** are given in the ESI.†

Synthesis of triazoles 8a–8d by using catalyst 3. Syntheses of **8a–8d** were accomplished by the same method as that described (neat conditions) for the other triazoles **7a–7l** by employing the corresponding azide and internal-terminal alkynes; however, the purification is as follows: the crude reaction mixture was purified by silica gel column chromatography using a 30% EtOAc/hexane mixture. After purification, the triazole derivatives bearing alkyne-phenyl propargylic ether substituents were isolated as yellow to orange semi-sticky solids in good to excellent yields (67–90%). The spectral data (^{1}H, ^{13}C, and HRMS) and yields are given in the ESI.†

Synthesis of 8e by using catalyst 3. The triazole **8e** was isolated as a pale yellow solid by following the procedure described for **7a–7l**. Yield: 57 mg (87%). ^{1}H NMR (700 MHz, CDCl$_3$): δ = 8.06 (d, *J* = 7.6 Hz, 2H), 7.42–7.37 (m, 2H), 7.33 (d, *J* = 8.5 Hz, 2H), 7.29–7.27 (m, 2H), 7.23 (t, *J* = 7.4 Hz, 2H), 7.12 (d, *J* = 8.0 Hz, 2H), 4.82 (s, 4H, NCH$_2$CH$_2$N), 4.48 (s, 2H, OCH$_2$), and 3.96 (s, 2H, OCH$_2$). ^{13}C NMR (176 MHz, CDCl$_3$): δ = 139.9, 134.7, 133.1, 128.8, 126.3, 123.1, 121.1, 120.7, 119.9, 107.9, 85.8 (*C≡C*), 85.5 (*C≡C*), 62.5 (OCH$_2$), 57.5 (OCH$_2$), 43.4 (NCH$_2$CH$_2$N), and 31.7 (NCH$_2$CH$_2$N). Mass spectral data (HRMS, CH$_3$CN, *m/z*): found 441.1461; calcd for C$_{26}$H$_{22}$ClN$_4$O; 441.1482 [M + H]$^+$. IR (ATR mode, cm^{-1}): 1599, 1485, 1451, 1330, 1222, 1073, 921, 823, 748, 718, and 524.

Synthesis of 9a by using catalyst 3.
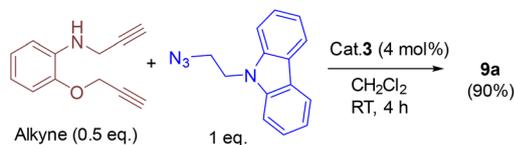
A 25 mL Schlenk tube was charged with carbazolyl azide (2 equiv.), bis-terminal alkyne (1 equiv.) and cat. **3** (4 mol%) under a nitrogen atmosphere. To this solid mixture, CH$_2$Cl$_2$ was added and stirred for 4 h at RT. A white precipitate formed was filtered and washed with CH$_2$Cl$_2$ (2 × 3 mL), followed by *n*-hexane (2 × 3 mL). The resulting solid was dried under vacuum to afford **9a** as a pale brown solid. Yield: 75 mg (90%). ^{1}H NMR (400 MHz, DMSO-d$_6$): δ = 8.10 (d, *J* = 8.0 Hz, 5H), 7.77 (s, 1H), 7.34 (m, *J* = 18.5, 8H), 7.16 (m, 4H), 6.87 (d, *J* = 7.7 Hz, 1H), 6.73 (t, *J* = 7.4 Hz, 1H), 6.52 (t, *J* = 7.4 Hz, 1H), 6.43 (d, *J* = 7.5 Hz, 1H), 4.98 (s, 3H), 4.90–4.66 (m, 8H), and 4.19 (d, *J* = 4.5 Hz, 2H). ^{13}C NMR (101 MHz, DMSO-d$_6$): δ = 145.1, 143.1, 139.8, 137.6, 125.7, 125.61, 124.9, 122.2, 122.1, 121.5, 120.2, 120.16, 119.1, 119.0, 115.9, 111.3, 109.7, 108.8, 108.7, 61.5 (OCH$_2$), 48.4 (NCH$_2$CH$_2$), 48.4 (NCH$_2$CH$_2$), 42.9 (NCH$_2$CH$_2$), 42.8 (NCH$_2$CH$_2$), and 38.5 (HNCH$_2$–). Melting point: 211 °C (decomposed to black solid). HRMS (MeOH, *m/z*): 658.3066; calcd for C$_{40}$H$_{36}$N$_9$O; 658.3043 [M + H]$^+$. IR (ATR mode, cm^{-1}): 3051, 1598, 1516, 1452, 1331, 1214, 1130, 1046, 1016, 847, 745, 666, 615, and 561.

Synthesis of 9b by using catalyst 3.
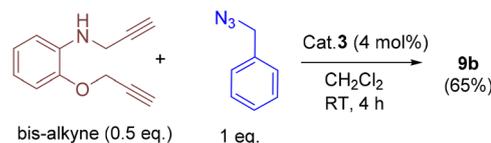
To a Schlenk tube containing benzyl azide (2 equiv.), bis-terminal alkyne (1 equiv.), and cat. **3** (4 mol%) was added CH$_2$Cl$_2$ (1 mL) and the mixture was stirred for 4 h at RT. The solvent was removed under reduced pressure, and it was further purified by flash column (silica gel) chromatography using ethyl acetate (15 mL). After the removal of the solvent, the residue was washed again with *n*-hexane (4 mL), and dried under vacuum to afford **9b** as a yellow oily substance. Yield: 44 mg (65%). ^{1}H NMR (400 MHz, CDCl$_3$): δ = 7.53 (s, 1H), 7.33 (m, 9H, ArH), 7.24–7.20 (m, 3H, ArH), 6.94–6.81 (m, 2H, ArH), 6.64 (dd, *J* = 7.9 Hz, 2H, ArH), 5.51 (s, 2H, BnCH$_2$), 5.46 (s, 2H, BnCH$_2$), 5.18 (s, 2H, OCH$_2$), and 4.42 (s, 2H, HNCH$_2$). ^{13}C NMR (101 MHz, CDCl$_3$): δ = 147.1, 145.8, 144.6, 138.1, 134.8, 134.6, 129.3, 128.8, 128.9, 128.8, 128.2, 128.1, 123.0, 122.3, 121.8, 117.3, 112.1, 110.96, 62.8 (OCH$_2$), 54.4 (BnCH$_2$), 54.3 (BnCH$_2$), and 39.9 (HNCH$_2$). HRMS (ESI, MeOH, *m/z*): 452.2208; calcd for C$_{26}$H$_{26}$N$_7$O: 452.2199 [M + H]$^+$. IR (ATR mode, cm^{-1}): 3052, 1600, 1511, 1449, 1334, 1262, 1208, 1122, 1048, 900, 847, 805, and 732.

Author contributions

AD supervised the project work. AKS prepared the metal complexes and carried out all the experiments. BD helped in substrate synthesis. All authors contributed to writing the manuscript. SJP and CP performed the X-ray diffraction analysis.

Conflicts of interest

There are no conflicts to declare.

Acknowledgements

References

1 (a) H. Shet, U. Parmar, S. Bhilare and A. R. Kapdi, *Org. Chem. Front.*, 2021, **8**, 1599–1656; (b) K. Izod, *Coord. Chem. Rev.*, 2013, **257**, 924–945; (c) A. Doddi, M. Peters and M. Tamm, *Chem. Rev.*, 2019, **119**, 6994–7112; (d) F. Buß, P. Mehlmann, C. Mück-Lichtenfeld, K. Bergander and F. Dielmann, *J. Am. Chem. Soc.*, 2016, **138**, 1840–1843.

2 G. Bouhadir and D. Bourissou, *Chem. Soc. Rev.*, 2016, **45**, 1065–1079.

3 T. Komuro, Y. Nakajima, J. Takaya and H. Hashimoto, *Coord. Chem. Rev.*, 2022, **473**, 214837.

4 L. Denker, D. Wullschläger, J. P. Martínez, S. Świerczewski, B. Trzaskowski, M. Tamm and R. Frank, *ACS Catal.*, 2023, **13**, 2586–2600.

5 P. Gualco, S. Ladeira, K. Miqueu, A. Amgoune and D. Bourissou, *Angew. Chem., Int. Ed.*, 2011, **50**, 8320–8324.

6 A. A. Omaña, R. K. Green, R. Kobayashi, Y. He, E. R. Antoniuk, M. J. Ferguson, Y. Zhou, J. G. C. Veinot, T. Iwamoto, A. Brown and E. Rivard, *Angew. Chem.*, 2021, **133**, 230–233.

7 C. A. Theulier, Y. García-Rodeja, S. Mallet-Ladeira, K. Miqueu, G. Bouhadir and D. Bourissou, *Organometallics*, 2021, **40**, 2409–2414.

8 C. A. Theulier, Y. García-Rodeja, N. Saffon-Merceron, K. Miqueu, G. Bouhadir and D. Bourissou, *Chem. Commun.*, 2021, **57**, 347–350.

9 D. Quintard, M. Keller and B. Breit, *Synthesis*, 2004, 905–908.

10 A. Kawachi, T. Yoshioka and Y. Yamamoto, *Organometallics*, 2006, **25**, 2390–2393.

11 J. Wen, B. Dong, J. Zhu, Y. Zhao and Z. Shi, *Angew. Chem., Int. Ed.*, 2020, **59**, 10909–10912.

12 (a) R. Imayoshi, K. Nakajima, J. Takaya, N. Iwasawa and Y. Nishibayashi, *Eur. J. Inorg. Chem.*, 2017, **2017**, 3769–3778; (b) F. Montilla, A. Galindo, V. Rosa and T. Aviles, *Dalton Trans.*, 2004, 2588–2592.

13 G. Chang, P. Zhang, W. Yang, Y. Dong, S. Xie, H. Sun, X. Li, O. Fuhr and D. Fenske, *Dalton Trans.*, 2021, **50**, 17594–17602.

14 S. Ren, S. Xie, T. Zheng, Y. Wang, S. Xu, B. Xue, X. Li, H. Sun, O. Fuhr and D. Fenske, *Dalton Trans.*, 2018, **47**, 4352–4359.

15 X.-L. Pei, A. Pereira, E. S. Smirnova and A. M. Echavarren, *Chem. – Eur. J.*, 2020, **26**, 7309–7313.

16 (a) R. Declercq, G. Bouhadir, D. Bourissou, M.-A. Légaré, M.-A. Courtemanche, K. S. Nahi, N. Bouchard, F.-G. Fontaine and L. Maron, *ACS Catal.*, 2015, **5**, 2513–2520; (b) M. Boudjelel, E. D. Sosa Carrizo, S. Mallet-Ladeira, S. Massou, K. Miqueu, G. Bouhadir and D. Bourissou, *ACS Catal.*, 2018, **8**, 4459–4464; (c) M. Boudjelel, S. Mallet-Ladeira, G. Bouhadir and D. Bourissou, *Chem.Comm.*, 2019, **55**, 12837–12840.

17 B. Ghaffari, S. M. Preshlock, D. L. Plattner, R. J. Staples, P. E. Maligres, S. W. Krska, R. E. Maleczka and M. R. Smith, *J. Am. Chem. Soc.*, 2014, **136**, 14345–14348.

18 (a) H. Kameo, J. Yamamoto, A. Asada, H. Nakazawa, H. Matsuzaka and D. Bourissou, *Angew. Chem., Int. Ed.*, 2019, **58**, 18783–18787; (b) F. Ritter, L. John, T. Schindler, J. P. Schroers, S. Teeuwen and M. E. Tauchert, *Chem. – Eur. J.*, 2020, **26**, 13436–13444.

19 (a) A. Marker and M. J. Gunter, *J. Magn. Reson.*, 1982, **47**, 118–132; (b) R. J. Bowen, M. Navarro, A.-M. J. Shearwood, P. C. Healy, B. W. Skelton, A. Filipovska and S. J. Berners-Price, *Dalton Trans.*, 2009, 10861–10870; (c) J. V. Hanna, S. E. Boyd, P. C. Healy, G. A. Bowmaker, B. W. Skelton and A. H. White, *Dalton Trans.*, 2005, 2547–2556.

20 S. M. Socol, R. A. Jacobson and J. G. Verkade, *Inorg. Chem.*, 1984, **23**, 88–94.

21 S. M. Socol and J. G. Verkade, *Inorg. Chem.*, 1984, **23**, 3487–3493.

22 R. E. Bachman and D. F. Andretta, *Inorg. Chem.*, 1998, **37**, 5657–5663.

23 A. Doddi, D. Bockfeld, A. Nasr, T. Bannenberg, P. G. Jones and M. Tamm, *Chem. – Eur. J.*, 2015, **21**, 16178–16189.

24 C. Zovko, S. Bestgen, C. Schoo, A. Görner, J. M. Goicoechea and P. W. Roesky, *Chem. – Eur. J.*, 2020, **26**, 13191–13202.

25 A. Doddi, M. Peters, D. Bockfeld and M. Tamm, *Z. Anorg. Allg. Chem.*, 2023, **649**, e202200364.

26 M. R. Churchill and K. L. Kalra, *J. Am. Chem. Soc.*, 1973, **95**, 5772–5773.

27 A. Bayler, A. Schier, G. A. Bowmaker and H. Schmidbaur, *J. Am. Chem. Soc.*, 1996, **118**, 7006–7007.

28 M. Altaf and H. Stoeckli-Evans, *Polyhedron*, 2010, **29**, 701–708.

29 M. Nazish, H. Bai, C. M. Legendre, R. Herbst-Irmer, L. Zhao, D. Stalke and H. W. Roesky, *Chem. Commun.*, 2022, **58**, 12704–12707.

30 (a) A. J. Blake, N. R. Brooks, N. R. Champness, J. W. Cunningham, P. Hubberstey and M. Schroeder, *CrystEngComm*, 2000, **2**, 41–45; (b) L. Poorters,

D. Armspach, D. Matt, L. Toupet and P. G. Jones, *Angew. Chem., Int. Ed.*, 2007, **46**, 2663–2665.

31 R. Kumar, S. Kumar, M. K. Pandey, V. S. Kashid, L. Radhakrishna and M. S. Balakrishna, *Eur. J. Inorg. Chem.*, 2018, **2018**, 1028–1037.

32 H. Wu, Y. Qu, C. Wang, Y. Wu and K. Zhao, *Phosphorus, Sulfur Silicon Relat. Elem.*, 2020, **195**, 88–95.

33 W. E. Slinkard and D. W. Meek, *Inorg. Chem.*, 1969, **8**, 1811–1816.

34 V. Montiel-Palma, M. A. Muñoz-Hernández, T. Ayed, J.-C. Barthelat, M. Grellier, L. Vendier and S. Sabo-Etienne, *Chem. Commun.*, 2007, 3963–3965.

35 S. Xu, P. Zhang, X. Li, B. Xue, H. Sun, O. Fuhr and D. Fenske, *Chem. – Asian J.*, 2017, **12**, 1234–1239.

36 U. Prieto-Pascual, A. Rodríguez-Diéguez, Z. Freixa and M. A. Huertos, *Inorg. Chem.*, 2023, **62**, 3095–3105.

37 M. Meldal and C. W. Tornøe, *Chem. Rev.*, 2008, **108**, 2952–3015.

38 L. Liang and D. Astruc, *Coord. Chem. Rev.*, 2011, **255**, 2933–2945.

39 B. Das, A. K. Sahoo, S. K. Banjare, S. J. Panda, C. S. Purohit and A. Doddi, *Dalton Trans.*, 2023, DOI: **10.1039/D3DT01989F**.

40 D. Wang, N. Li, M. Zhao, W. Shi, C. Ma and B. Chen, *Green Chem.*, 2010, **12**, 2120–2123.

41 S. Lal, J. McNally, A. J. P. White and S. Díez-González, *Organometallics*, 2011, **30**, 6225–6232.

42 (*a*) L. Li and Z. Zhang, *Molecules*, 2016, **21**, 1393; (*b*) Y.-C. Lin, Y.-J. Chen, T.-Y. Shih, Y.-H. Chen, Y.-C. Lai, M. Y. Chiang, G. C. Senadi, H.-Y. Chen and H.-Y. Chen, *Organometallics*, 2019, **38**, 223–230.

43 B. T. Worrell, J. A. Malik and V. V. Fokin, *Science*, 2013, **340**, 457–460.

44 F. Himo, T. Lovell, R. Hilgraf, V. V. Rostovtsev, L. Noodleman, K. B. Sharpless and V. V. Fokin, *J. Am. Chem. Soc.*, 2005, **127**, 210–216.

45 P. Mathew, A. Neels and M. Albrecht, *J. Am. Chem. Soc.*, 2008, **130**, 13534–13535.

46 C. Nolte, P. Mayer and B. F. Straub, *Angew. Chem., Int. Ed.*, 2007, **46**, 2101–2103.

47 E. Fossum, Z. Yu and L.-S. Tan, *ARKIVOC*, 2010, **2009**, 255–265.